8-4-2021

The impact of alkali-ion intercalation on redox chemistry and mechanical deformations: Case study on intercalation of Li, Na, and K ions into FePO4 cathode

Bertan Özdogru

Behrad Koohbor
Rowan University, koohbor@rowan.edu

O. Ozgur Capraz

Recommended Citation

B. Özdogru, B. Koohbor, Ö. Ö. Çapraz. The impact of alkali-ion intercalation on redox chemistry and mechanical deformations: Case study on intercalation of Li, Na, and K ions into FePO4 cathode. Electrochem. Sci. Adv. 2021, e2100106. https://doi.org/10.1002/elsa.202100106

Short communication
doi.org/10.1002/elsa.202100106

Chemistry Europe
European Chemical Societies Publishing

Received: 27 May 2021
Revised: 29 June 2021
Accepted: 4 August 2021

The impact of alkali-ion intercalation on redox chemistry and mechanical deformations: Case study on intercalation of Li, Na, and K ions into $FePO_4$ cathode

Bertan Özdogru[1] | **Behrad Koohbor**[2] | **Ö. Özgür Çapraz**[1]

[1] The School of Chemical Engineering, Oklahoma State University, Stillwater, Oklahoma, USA

[2] Department of Mechanical Engineering, Rowan University, Glassboro, New Jersey, USA

Correspondence
Ö. Ö. Çapraz, The School of Chemical Engineering, Oklahoma State University, Stillwater, OK 74078.
Email: ocapraz@okstate.edu

Funding information
U.S. Department of Energy, Office of Science; Basic Energy Sciences, Grant/Award Number: DE-SC0021251

Abstract

Batteries made of charge carriers from Earth-crust abundant materials (e.g., Na, K, and Mg) have received extensive attention as an alternative to Li-ion batteries for grid storage. However, a lack of understanding of the behavior of these larger ions in the electrode materials hinders the development of electrode structures suitable for these large ions. In this study, we investigate the impact of alkali ions (Li, Na, and K) on the redox chemistry and mechanical deformations of iron phosphate composite cathodes by using electrochemical techniques and in situ digital image correlation. Na-ion and Li-ion intercalation demonstrate a nearly linear correlation between electrochemical strains and the state of charge and discharge. The strain development shows nonlinear dependance on the state of charge and discharge for K ions. Strain rate calculations show that K ion intercalation results in a progressive increase in the strain rate for all cycles. Li and Na intercalation induce nearly constant strain rates with the exception of the first discharge cycle of Na intercalation. When the same amount of ions are inserted into the electrode, the electrode shows the lowest strain generation upon Li intercalation compared to larger alkali ions. Na and K ions induce similar volumetric changes in the electrode when the state of charge and discharge is around 30%. Although the electrode experiences larger absolute strain generation at the end of the discharge cycles upon Na intercalation, strain rates were found to be greater for K ions. Potential-dependent behaviors also demonstrate more sluggish redox reactions during K intercalation, compared to Li and Na. Our quantitative analysis suggests that the strain rate, rather than the absolute value of strain, is the critical factor in amorphization of the crystalline electrode.

KEYWORDS
alkali-ions, chemomechanics, electrochemical strains, Iron phosphate, K-ion, Li-ion, Na-ion, sluggish reactions

Short communication
doi.org/10.1002/elsa.202100106
Chemistry Europe
European Chemical Societies Publishing

1 | INTRODUCTION

Development of cathode structures suitable for Na-ion and K-ion batteries is still one of the major challenges on the way to the design of next-generation alkali metal-ion batteries. Although Li, Na, and K belong to the same alkali metal group with a single charge in their cation form, intercalation of Na^+ and K^+ ions in electrodes is difficult since ionic radii of Na^+ (1.02 Å) and K^+ (1.38 Å) are larger than that of Li^+ (0.76 Å).[1] Therefore, physical and electrochemical behavior of the cathode materials in response to Na^+ and K^+ ion intercalation is expected to be fundamentally different from the response to Li^+ ion. However, there is not much known about how electrochemical reactions and the transport of ions that take place in cathode materials with different alkali metal ions. There have been several studies focusing on electrochemical characterization and investigation of the structural changes in the electrode materials.[2–7] A lack of insight into these reaction-transport mechanisms limits the design of novel cathode materials for Na-ion and K-ion batteries. Therefore, comparative studies between Li-ion, Na-ion, and K-ion battery cathodes are critical to identify fundamental similarities and differences during intercalation.

Even modest expansions in brittle cathodes can cause particle fracturing in a larger crystalline-size scale.[8–12] Intercalation of larger ions can cause structural collapse and amorphization induced by continuous accumulation of strains and distortions.[13–15] Dislocation activity has been observed during electrochemical delithiation of micron size $LiFePO_4$ particles, although the lattice strains were only around 5% for $LiFePO_4$.[16] Synchrotron radiation powder X-ray diffraction and pair distribution function analysis demonstrated the formation of amorphous phases in iron phosphate electrodes during Na intercalation.[11] Islam *et al*[17] discussed the effect of lattice strain on the ion condition and defect properties of $LiFePO_4$ and $NaFePO_4$ using atomistic simulations. The calculations suggest that tensile strains generated perpendicularly to the migration channels can improve the intercalation kinetics in polyanionic compounds cathodes.[17] Lattice strain induced by large Na^+ ion intercalation into Na_xCuS structure causes crystallographic tuning and deviation of reaction pathways from the thermodynamic equilibrium.[18] K^+ ion insertion into $FePO_4$ electrode resulted in amorphization or severe crystallinity lowering in crystalline $FePO_4$ electrode.[19] Amorphization of layered manganese oxide ($AMnO_2$) is also observed upon Na^+ and K^+ ion intercalation.[13] Recent TEM studies show a slight amorphization in the iron phosphate electrode upon Na intercalation,[11] whereas K ions cause amorphization in the crystal structure of iron phosphate.[20] Although the amorphization in the structure can be easily identified by conventional diffraction or electron microscopy techniques, quantitative analysis of the physical changes in the structure during and after amorphization while cycling the battery electrode is critical. Recently, we developed a new experimental approach to monitor dynamic physical and structural changes in the amorphous phase of the electrodes by combining *in situ* strain measurements via digital image correlation (DIC) and in-operando XRD techniques.[21] The study detected the redox chemistry and the associated electrochemical strains in the amorphous phases of the iron phosphate electrode during K ion intercalation.[21]

In this work, we compare the *operando* physical and electrochemical responses of the host cathode electrode upon intercalation of Li, Na, and K ions using DIC and electrochemical methods. Iron phosphate was selected as a model system because it allows intercalation of Li, Na, and K ions.[22,23] Chemomechanical strains were observed to increase linearly with Li and Na intercalation. However, strain development shows a nonlinear increase with K intercalation. Strain rates were more constant and lower in value during Li intercalation. Our study provides a quantitative analysis into the electrochemical strains causing irreversible deformations in the crystalline iron phosphate electrode. More importantly, we show that although the net value of electrochemical strains are similar with Na and K ion intercalation, the kinetics of strain development is different for various ions.

2 | MATERIALS AND METHODS

Composite electrodes were prepared by mixing pristine lithium iron phosphate ($LiFePO_4$, LFP, Hanwha Chemical) with sodium carboxymethyl cellulose (binder, CMC, Aldrich) and conductive additive (carbon black, Alfa Aesar) in 8:1:1 mass ratio. Iron phosphate ($FePO_4$, FP) composite electrode was formed by electrochemical displacement technique using a pristine LFP composite electrode[21–24] via galvanostatic cycle at a rate of C/10. $FePO_4$ electrodes were charged and discharged with Li, Na, or K ions by galvanostatic cycles at C/25 rate against Li, Na, or K counter electrodes, respectively. The iron phosphate electrodes were charged and discharged at C/25 rate, based on a theoretical capacity of 170 mAh/g for $LiFePO_4$, 154 mAh/g for $NaFePO_4$, and 131 mAh/g for $KFePO_4$. The following salts and solvents were used to prepare electrolytes: 1 M $LiClO_4$ in 1:1 (v/v) EC:DMC for Li intercalation and 1 M $NaClO_4$ in 1:1 (v/v) EC:DMC for Na intercalation. Note that 0.5 M KPF_6 in 1:1 (v/v) EC:DMC or EC:PC electrolytes were used for K intercalation. DIC technique was used to probe in situ strain generation during battery cycling. The natural surface features of

Short communication
doi.org/10.1002/elsa.202100106
Chemistry Europe
European Chemical Societies Publishing

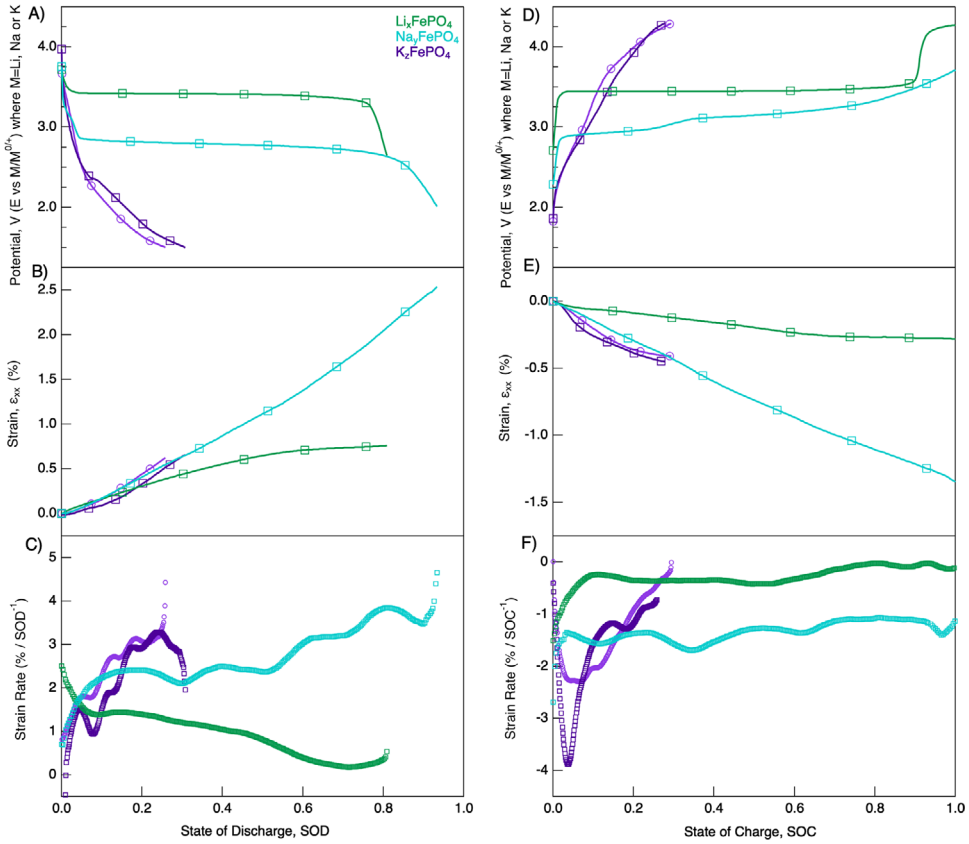

FIGURE 1 Potential evolution, strain generation and strain rates with respect to state of discharge (A, B, C) and charge (D, E, F) of Li (green), Na (blue), and K (purple) ions into $FePO_4$ electrode during the first cycle. The square and spherical symbol show when electrode is cycled either in EC:DMC or EC:PC solvents, respectively. Strain set to zero at the beginning of each charge/discharge cycles

the composite electrode were used as a speckle pattern suitable for the calculations of displacement fields and their resultant strain distribution on the electrode surface. A detailed description of the technique and custom battery cell was provided in our previous publication.[25]

3 | RESULTS AND DISCUSSION

3.1 | First cycle

Li, Na, and K ions are intercalated into iron phosphate electrode at C/25 rate while monitoring in situ strain generation in the electrode. Voltage and electrochemical strains during the first cycle are plotted against the state of discharge (SOD) or state of charge (SOC) during Li, Na, and K ions intercalation and de-intercalation, respectively. (Figure 1). SOD/SOC is calculated by dividing practical capacity measured in the experiment by theoretical capacity of $LiFePO_4$, $LiFePO_4$, or $KFePO_4$. A single voltage plateau is observed during Li and Na intercalation into iron phosphate at around 3.41V (vs $Li/Li^{0/+}$) and 2.81V (vs $Na/Na^{0/+}$), respectively. A two-phase reaction between iron phosphate and $LiFePO_4$ or $NaFePO_4$ results in a single potential plateau during the galvanostatic discharge cycles.[22,23] The $LiFePO_4$ electrode showed a flat potential plateau around 3.44 V versus $Li/Li^{0/+}$. $NaFePO_4$ electrode showed two distinct plateaus at around 2.93 and 3.21 V versus $Na/Na^{0/+}$. The two potential plateaus during desodiation are attributed to the formation of $Na_{0.7}FePO_4$ reaction intermediate during transition of $NaFePO_4$ phase to $FePO_4$ phase.[22] In the case of K intercalation/de-intercalation, potential profiles did not show any distinct plateau during intercalation of K ions into iron phosphate. Similar potential evolution in two different electrolyte systems ensures that the electrochemical behavior is due to K-ion intercalation/de-intercalation in the electrode. Also, a similar potential profile was reported when K ions were intercalated into amorphous iron phosphate.[26] A recent in situ XRD study also demonstrated the amorphization of the crystalline iron phosphate during the intercalation of K ions.[21]

The corresponding electrochemical strains in the electrodes upon Li, Na, and K intercalation are shown in Figure 1B and E. The electrode expanded by almost 0.65% and 2.53% at the end of the first discharge of Li and Na ions,

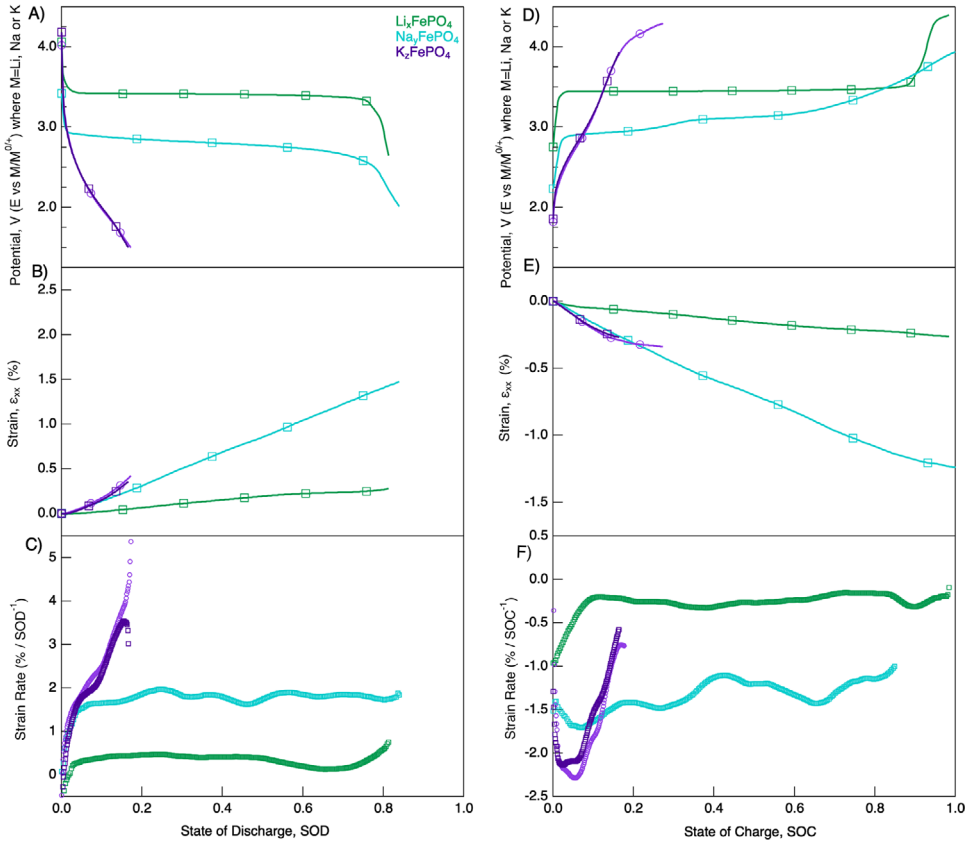

FIGURE 2 Potential evolution, strain generation and strain rates with respect to state of discharge (A,B, C) and charge (D, E, F) of Li (green), Na (blue), and K (purple) ions into $FePO_4$ electrode during the fourth cycle. The square and spherical symbol show when electrode is cycled either in EC:DMC or EC:PC solvents, respectively

respectively. K ions were only able to intercalate into electrode structure up to an SOD of ca. 0.30, resulting in 0.15% strain generation. In the case of charge reactions, extraction of Li and Na ions from $LiFePO_4$ and $NaFePO_4$ resulted in –0.30 and –1.21% contraction. During the removal of K ions, potassium iron phosphate experienced –0.40% reduction in the electrochemical strains at 0.3 SOD. The electrode experiences –0.12, and –0.40% strain generation at 0.3 SOD during Li and Na ion intercalation. The $NaFePO_4$ and K_zFePO_4 electrodes undergo similar strain generation when the same amount of Na or K ions were removed from or inserted into $NaFePO_4$ and K_zFePO_4 electrodes, respectively. Overall, the slope of strain build up changes dramatically during K ion intercalation, whereas strain evolutions during Li intercalation show a lower degree of nonlinearity during the first discharge cycle only. The slope of strains increased during Na ion insertion, however strain rate become constant during Na extraction in the first cycle.

Since SOD/SOC during discharge and charge of K ions was less than 0.35, Figure S1 is limited to 0.35 SOC/SOD for better comparison between Li, Na, and K intercalation behavior during the first cycle. The slope of the strains was progressively increased as more potassium ions were intercalated into the electrode. We determined strain rates during charge and discharge cycles by calculating the derivative of electrochemical strains with respect to the SOD/SOC. Between 0.05 and 0.35 of SOD, the strain rates for Li and Na intercalation into iron phosphate were about 1.40 and 2.40 %-SOD^{-1}, respectively. Strain rate during Na ion intercalation become around 3.5%-SOD^{-1}at the end of the discharge. On the other hand, the strain rates continuously increased as more K ions were intercalated into iron phosphate and reached to around 3.2 %-SOD^{-1} when the voltage reached 1.5V versus $K/K^{0/+}$ at the end of the discharge cycle. During the first charge, strain rates drastically reduced from about -3 %-SOC^{-1} to almost 0.5%-SOC^{-1} during K extraction from K_zFePO_4. On the other hand, extraction of Na and Li from $NaFePO_4$ and $LiFePO_4$ shows constant strain rates at around -0.35 and -1.35 %-SOC^{-1}, respectively.

3.2 | Subsequent cycles

Figure 2 shows the voltage profile and strain generation during the fourth cycle. The second and third cycle data

Short communication
doi.org/10.1002/elsa.202100106
Chemistry Europe
European Chemical Societies Publishing

were also plotted in Figures S2–S6. Overall, the potential profiles during the subsequent charge/discharge cycle of Li, Na, and K ions show very similar behavior compared with the first cycles. A single potential plateau was observed during both charge and discharge of Li ions in $LiFePO_4$ cathode. Charge cycles during Na extraction showed two distinct potential plateaus and Na intercalation resulted in a single potential plateau in $NaFePO_4$. Again, potential profiles did not show any distinct plateaus during subsequent charge/discharge cycles of K ions in K_zFePO_4 cathode.

Electrochemical strains showed a nearly linear increase with Li and Na intercalation. However, strain generation data showed nonlinear increase during K ion intercalation into K_zFePO_4. Na and K intercalation resulted in much larger electrochemical strains in the electrode compared to the Li intercalation due to their comparably larger ion sizes. It is interesting that the electrode experiences almost the same amount of strain generation during Na and K ion intercalation when the same number of ions are inserted into or removed from the electrode structure. We, again, calculated the strain rates during Li, Na, and K intercalation into the electrode structure. Similar to the first cycle, the strain rate continuously increased during K ion intercalation at the fourth discharge cycle. However, the values of calculated strain rates were almost constant during charge/discharge cycles of Li and Na ions in the electrode. Strain rates during K ion intercalation clearly demonstrated a major difference in comparison with strain rates during Li and Na intercalation into iron phosphate electrode.

Overall, lithium intercalation into the iron phosphate results in the least strain generation in the electrode structure compared to the Na^+ ion and K^+ ion intercalation. This behavior was expected as the Li ions is the smallest in ionic size, therefore results in less expansion in the crystalline structure during discharge. During the first discharge, Na ion intercalation in the crystalline iron phosphate resulted in a steady increase in strain rate, which becomes almost 3.5%-SOD^{-1} at the end of the first discharge. Surprisingly, the rate of strains at the end of the first discharge was very similar upon Na and K ion intercalation. In the subsequent cycles, Na-ion intercalation cause much larger strains in the electrode due to larger discharge capacities in comparison with K-ion intercalation. The strain rates were almost constant around 2%-SOD^{-1} in the subsequent discharge cycles during Na insertion. This is quite interesting behavior. Previously, Xiang et al.[11] reported a loss of crystallinity in the iron phosphate electrode during the first discharge cycle by *in situ* XRD measurements supported by ex situ TEM analysis. They associated the loss of crystallinity in the first discharge cycle to the formation of amorphous phases in the iron phosphate electrode. Beyond the first discharge cycle, their XRD analysis demonstrated the preservation of crystallinity in the iron phosphate electrode.[11] This study is well-aligned with our results with the progressive strain rate evolution only observed during the first discharge of Na ion intercalation. In the case of K ion intercalation, the steady increase in the strain rates are observed in the subsequent cycles too. XRD studies on K ion intercalation into iron phosphate demonstrated amorphization in the crystalline structure.[19,21] Therefore, progressive evolution of the strain rates in the electrodes is likely due to the occurrence of plastic deformation in the electrode structure. Constant strain rates during Li and Na intercalation can be interpreted as preserving crystalline structure while removing these ions from the host structure. Sharp changes in strain rates during K insertion and removal from the electrode results in an SOC (discharge) dependent nonlinear strain evolution and deformations in the electrode.

3.3 | Potential-dependent mechanical behavior

To further elucidate the difference between the electrochemical deformation behaviors observed in the electrodes, we further investigated the redox chemistry and associated mechanical deformations in the electrode. Capacity and strain derivatives in the $FePO_4$ electrode during Li, Na, and K intercalation were calculated to evaluate electrochemical reaction processes and structural changes in the electrode. The derivatives in the first two cycles are shown in Figure 3. Strain and capacity derivatives during the third and fourth cycles are shown in Figure S7. The electrochemical potentials in Na and K ion batteries were measured against the reduction potential of Na and K metals.

Capacity and strain derivative analyses demonstrated the fundamental differences in intercalation mechanism of Li-ion, Na-ion, and K-ion into iron phosphate. During Li and Na intercalation, the shape and location of strain derivative curves are almost identical to the capacity derivatives during the four cycles. Capacity and strain derivative peaks during Li and Na intercalation occurred at potentials where redox reactions and associated phase transformations in the electrode structure have been reported before.[22,23] Reversible behavior of the derivatives in each cycle suggests that the redox potentials do not change significantly over the subsequent cycles. Li-ion intercalation took place in a narrow potential range as demonstrated by sharp capacity and strain derivatives in Figure 3. The observation of broader peaks in capacity and strain derivatives during Na-ion intercalation

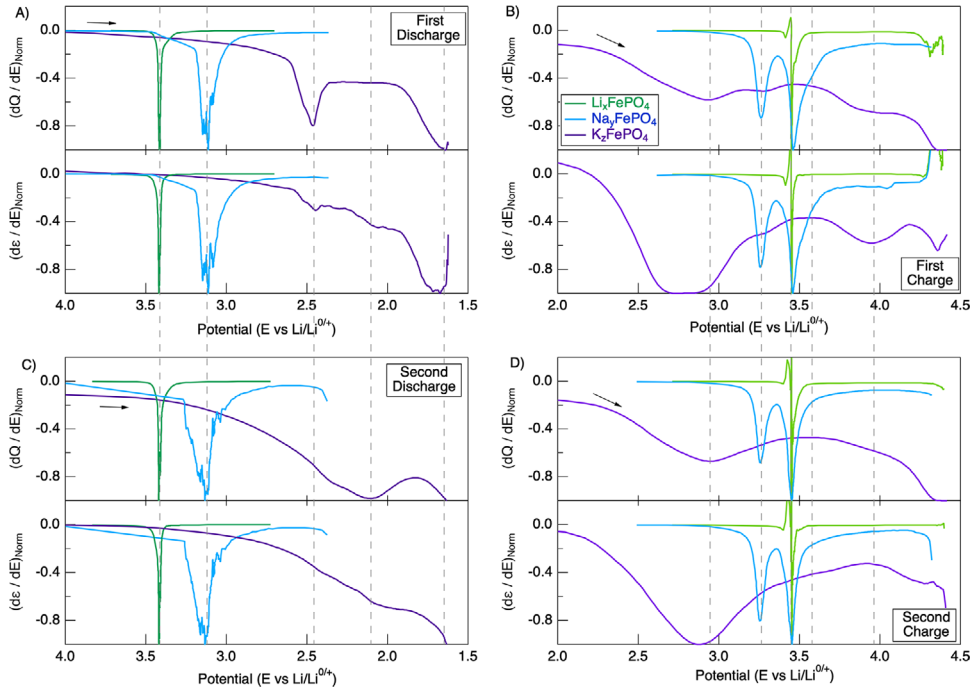

FIGURE 3 Normalized derivatives of capacity (dQ/dE) and strains ($d\varepsilon/dE$) with respect to potential for intercalation of Li (green), Na (blue), and K (purple) ions into $FePO_4$ during first (A, B) and second (C, D) discharge and charge cycles. Derivatives are normalized by dividing the maximum nominal values in each charge and discharge cycles

suggests the slower intercalation in comparison to Li-ions. In the case of K ion intercalation, there was a significant difference in terms of the evolution of capacity and strain derivatives. First, irreversible derivative peaks of strain and capacity derivative peaks were observed during the first discharge of K ions at around 2.3 V and 1.55 V. In the subsequent discharge cycles, very broad capacity peaks were observed at around 1.9 V. Strain derivatives did not show any characteristic peaks except change in the rate of strain derivatives at around 1.9 V. This behavior suggests the structural resistance towards the intercalation of K-ions into iron phosphate. During the charge cycles and upon K ion extraction from the electrode, broad capacity and strain derivative peaks were observed at around 2.75 V during the extraction of K ions from the electrode. A well-defined and reversible derivative peak during extraction of K ions points to the slower reaction kinetics during the phase transformation in the electrode structure.

4 | CONCLUSION

In this work, we compared the electrochemical and mechanical response of the iron phosphate cathodes upon Li, Na, and K ion intercalation by using electrochemical techniques and *in situ* digital image correlation. Iron phosphate model electrodes were prepared by electrochemical displacement technique in order to ensure identical morphology, structure, and chemistry in the pristine iron phosphate electrodes. Strain evolution during Li and Na intercalation results in more linear dependence on the SOC/SOD with the exception of the first discharge cycle of Na ions. However, strains generated in the electrode shows nonlinear behavior during insertion and extraction of K ions. When the same amount of K and Na ions were intercalated, similar chemomechanical expansions were observed. When the same amount of ions are intercalated into the electrode, the least volumetric expansions were observed for Li-ion insertion. The electrode experienced larger magnitudes of strains upon Na ion intercalation at the end of discharge cycles. However, strain rate calculations showed that K ion intercalation results in a progressive increase in the strain rate, whereas Li and Na intercalation induce nearly constant strain rates. Potential-dependent behaviors also demonstrate more sluggish redox reactions during K intercalation, compared to the Li and Na intercalation. Our results shows that strain rates are critical factor for the amorphization of the crystalline structure, rather than the absolute value of electrochemical strains. These observations provide a fundamental insight into the impact of alkali ions on the redox chemistry and associated chemomechanical deformations.

ACKNOWLEDGMENTS

This work was supported by the U.S. Department of Energy, Office of Science, Basic Energy Sciences (Award number DE-SC0021251). The experiments and data analysis are performed at Oklahoma State University.

AUTHORS CONTRIBUTIONS

The manuscript was written through contributions of all authors. All authors have given approval to the final version of the manuscript. Ö. Ö. Ç conceived the idea and supervised the work. B. O. prepared cathode slurries and performed in situ strain measurements. All authors discussed the results. The authors declare that they have no competing interests. All data needed to evaluate the conclusions in the paper are present in the paper and/or the Supporting information. Additional data related to this paper may be requested from the authors.

DATA AVAILABILITY STATEMENT

All data needed to evaluate the conclusions in the paper are present in the paper and/or the Supporting information. Additional data related to this paper may be requested from the authors.

ORCID

Ö. Özgür Çapraz https://orcid.org/0000-0002-2396-4748

REFERENCES

1. J. G. Speight, *Lange's Handbook of Chemistry*, sixteenth, McGraw-Hill Education, **2005**.
2. D. Saurel, M. Galceran, M. Reynaud, H. Anne, M. Casas-Cabanas, *Int. J. Energy Res.* **2018**, *42*, 3258.
3. K. Walczak, A. Kulka, B. Gędziorowski, M. Gajewska, J. Molenda. *Solid State Ionics* **2018**, *319*, 186.
4. Y. Fang, J. Zhang, L. Xiao, X. Ai, Y. Cao, H. Yang, *Adv. Sci.* **2017**, *4*, 1600392.
5. Y. Zhu, Y. Xu, Y. Liu, C. Luo, C. Wang, *Nanoscale* **2013**, *5*, 780.
6. E. Memarzadeh Lotfabad, P. Kalisvaart, A. Kohandehghan, D. Karpuzov, D. Mitlin, *J. Mater. Chem. A* **2014**, *2*, 19685.
7. E. de la Llave, V. Borgel, K. J. Park, J. Y. Hwang, Y.-K. Sun, P. Hartmann, F.-F. Chesneau, D. Aurbach, *ACS Appl. Mater. Interfaces* **2016**, *8*, 1867.
8. K. Dokko, M. Nishizawa, S. Horikoshi, T. Itoh, M. Mohamedi, I. Uchida, *Electrochem. Solid-State Lett.* **1999**; *3*, 125.
9. D. Wang, X. Wu, Z. Wang, L. Chen, *J. Power Sources* **2005**, *140*, 125.
10. Z. Zhang, Z. Chen, G. Wang, H. Ren, M. Pan, L. Xiao, K. Wu, L. Zhao, J. Yang, Q. Wu, J. Shu, D. Wang, H. Zhang, N. Huo, J. Li, *Phys. Chem. Chem. Phys.* **2016**, *18*, 6893.
11. K. Xiang, W. Xing, D. B. Ravnsbæk, L. Hong, M. Tang, Z. Li, K. M. Wiaderek, O. J. Borkiewicz, K. W. Chapman, P. J. Chupas, Y.-M. Chiang, *Nano Lett.* **2017**, *17*, 1696.
12. A. Whiteside, C. A. J. Fisher, S. C. Parker, M. Saiful Islam, *Phys. Chem. Chem. Phys.* **2014**, *16*, 21788.
13. Z. Dai, U. Mani, H. T. Tan, Q. Yan, *Small Methods* **2017**, *1*, 1700098.
14. M. R. Bonilla, A. Lozano, B. Escribano, J. Carrasco, E. Akhmatskaya, *J. Phys. Chem. C* **2018**, *122*, 8065.
15. A. Saracibar, J. Carrasco, D. Saurel, M. Galceran, B. Acebedo, H. Anne, M. Lepoitevin, T. Rojo, M. Casas Cabanas, *Phys. Chem. Chem. Phys.* **2016**, *18*, 13045.
16. Y. Zhu, J. W. Wang, Y. Liu, X. Liu, A. Kushima, Y. Liu, Y. Xu, S. X. Mao, J. Li, C. Wang, J. Y. Huang, *Adv. Mater.* **2013**, *25*, 5461.
17. C. Tealdi, J. Heath, M. S. Islam, *J. Mater. Chem. A* **2016**, *4*, 6998.
18. J. Y. Park, S. J. Kim, J. H. Chang, H. K. Seo, J. Y. Lee, J. M. Yuk, *Nat. Commun.* **2018**, *9*, 1.
19. T. Hosaka, T. Shimamura, K. Kubota, S. Komaba, *Chem. Rec.* **2019**, *19*, https://doi.org/10.1038/s41467-018-03322-9.
20. K. Kubota, M. Dahbi, T. Hosaka, S. Kumakura, S. Komaba, *Chem. Rec.* **2018**, *18*, 459.
21. B. Ozdogru, Y. Cha, M. Vijayakumar, M.-K. Song, Ö. Ö. Capraz, *ChemRxiv. Prepr.* **2021**, https://doi.org/10.26434/chemrxiv.14579259.v1.
22. C. Heubner, S. Heiden, B. Matthey, M. Schneider, A. Michaelis, *Electrochim. Acta* **2016**, *216*, 412.
23. C. Heubner, S. Heiden, M. Schneider, A. Michaelis, *Electrochim. Acta* **2017**, *233*, 78.
24. B. Özdogru, H. Dykes, S. Padwal, S. Harimkar, Ö. Ö. Çapraz, B. Özdogru, H. Dykes, Ö. Ö. Çapraz, *Electrochim. Acta* **2020**, *353*, 136594.
25. Ö. Ö. Çapraz, S. Rajput, S. White, N. R. Sottos, *Exp. Mech.* **2018**, *58*, 561.
26. V. Mathew, S. Kim, J. Kang, J. Gim, J. Song, J. P. Baboo, W. Park, D. Ahn, J. Han, L. Gu, Y. Wang, Y.-S. Hu, Y.-K. Sun, J. Kim, *NPG Asia Mater.* **2014**, *6*, e138.

SUPPORTING INFORMATION

Additional supporting information may be found online in the Supporting Information section at the end of the article.

How to cite this article: B. Özdogru, B. Koohbor, Ö. Ö. Çapraz, *Electrochem. Sci. Adv.* **2021**, e2100106. https://doi.org/10.1002/elsa.202100106